

1-(β -D-Erythrofuranosyl)cytidine
(β -erythrocytidine)Paul C. Kline,^a Bruce C. Noll,^b Hongqiu Zhao^b and
Anthony S. Serianni^{b*}^aDepartment of Chemistry, Middle Tennessee State University, Murfreesboro,
TN 37132, USA, and ^bDepartment of Chemistry and Biochemistry, 251 Nieuwland
Science Hall, University of Notre Dame, Notre Dame, IN 46556-5670, USA
Correspondence e-mail: serianni.1@nd.edu

Received 16 October 2006

Accepted 18 December 2006

Online 23 January 2007

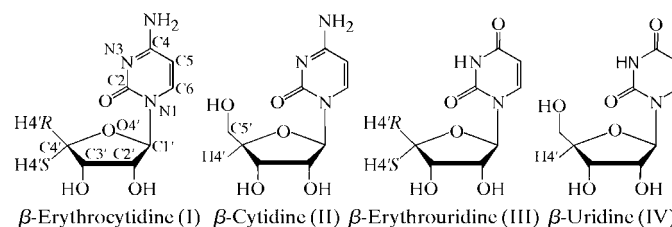
1-(β -D-Erythrofuranosyl)cytidine, C₈H₁₁N₃O₄, (I), a derivative of β -cytidine, (II), lacks an exocyclic hydroxymethyl (–CH₂OH) substituent at C4' and crystallizes in a global conformation different from that observed for (II). In (I), the β -D-erythrofuranosyl ring assumes an E_3 conformation (C3'-*exo*; *S*, *i.e.* south), and the N-glycoside bond conformation is *syn*. In contrast, (II) contains a β -D-ribofuranosyl ring in a 3T_2 conformation (*N*, *i.e.* north) and an *anti*-N-glycoside linkage. These crystallographic properties mimic those found in aqueous solution by NMR with respect to furanose conformation. Removal of the –CH₂OH group thus affects the global conformation of the aldofuranosyl ring. These results provide further support for *S*/*syn-anti* and *N*/*anti* correlations in pyrimidine nucleosides. The crystal structure of (I) was determined at 200 K.

Comment

Tetrofuranose-containing nucleosides and their phosphate esters have attracted attention recently as building blocks in the preparation of novel oligonucleotides (Schoning *et al.*, 2000; Kempeneers *et al.*, 2004). Oligonucleotides containing β -tetrofuranosyl rings, which lack the exocyclic C5' hydroxymethyl group found in β -ribofuranosyl rings, are necessarily assembled *via* 2'→3'-phosphodiester linkages. The *trans*-O2',O3' configuration found in *L-threo* derivatives (TNA) mimics backbones formed from conventional 3'→5' linkages (Wilds *et al.*, 2002), whereas the *cis*-O2',O3' configuration found in *erythro* building blocks presumably results in oligonucleotides with considerably different structures and topologies.

Nucleoside conformation in solution is affected significantly by removal of the furanose exocyclic hydroxymethyl functionality. NMR investigations of β -erythronucleosides have revealed very different J_{HH} , J_{CH} and J_{CC} values, indicative of a major shift in the preferred conformation of the furanose ring

relative to that observed in the corresponding β -ribonucleosides (Kline & Serianni, 1992). For example, the endocyclic ${}^3J_{H1',H2'}$, ${}^3J_{H2',H3'}$ and ${}^3J_{H3',H4'}$ values are 5.6, 4.6 and 3.3 Hz (to H4'*S*) in β -erythrocytidine, (I), whereas the corresponding values in β -cytidine, (II), are 3.9, 5.3 and 6.0 Hz, respectively. Pseudorotational analysis (Rao *et al.*, 1981) of these J couplings reveals a highly preferred *S* (south) furanose conformation in (I) (79%; $P = 186.4^\circ$ and $\tau_m = 40^\circ$), whereas a similar analysis for (II) reveals a preferred *N* (north) conformation (58%; $P = 21.8^\circ$ and $\tau_m = 38^\circ$) (Fig. 1). The different preferred furanose conformations were expected to affect N-glycoside conformation in (I) and (II), but NMR data were unavailable to address this question.



A comparison of the low-temperature crystal structure of (I) determined here (Fig. 2) with that of (II) (Ward, 1993) shows differences in furanose conformation nearly identical to those observed in solution. Removal of the exocyclic –CH₂OH group stabilizes *S* conformations, with E_3 (C3'-*exo*) preferred in (I) ($P = 197.8^\circ$ and $\tau_m = 44^\circ$) and 3T_2 preferred in (II) ($P = 7.7^\circ$ and $\tau_m = 39^\circ$) (Fig. 1 and Table 1). These results can be explained based on a preferred quasi-equatorial orientation of the bulkier –CH₂OH substituent in (II), which is achievable in *N* conformations like 3T_2 . While the pseudorotational phase angles, P , differ significantly, the puckering amplitudes, τ_m , are similar in (I) and (II) (Table 1). Endocyclic C1–C2 and C2–C3 bond lengths in (I) are larger by ~ 0.01 Å, whereas $r_{C3,C4}$ in (I) and (II) are more similar ($\Delta = 0.004$ Å) (Table 1).

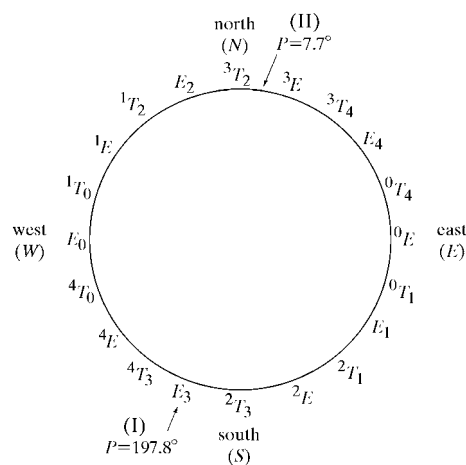


Figure 1

The pseudorotational itinerary of an aldofuranose ring. *E* and *T* denote envelope and twist forms, respectively. The preferred furanose conformations in crystalline (I) and (II) are highlighted.

The change in the furanose conformation caused by removal of the $-\text{CH}_2\text{OH}$ substituent is accompanied by a significant change in the N-glycoside conformation. In (I), the nitrogen base is oriented *syn/+sc*, with the $\text{C}2-\text{O}2$ bond oriented above the furanose ring, corresponding to an $\text{O}4'-\text{C}1'-\text{N}1-\text{C}2$ torsion angle of $60.8(2)^\circ$ (Table 1). In contrast, the N-glycoside conformation is *anti/ap* in (II) [$\text{O}4'-\text{C}1'-\text{N}1-\text{C}2$ torsion angle = $-162.6(3)^\circ$], orienting the $\text{C}6-\text{H}6$ bond above the furanose ring; the $\text{C}1'-\text{N}1$ bond is rotated almost 180° in (II) relative to (I). A correlation between the N-glycoside and furanose conformations is thus evident (Saenger, 1984). 3E conformations leave the top face of the furanose ring unhindered by the $-\text{CH}_2\text{OH}$ group, but the resulting quasi-axial orientation of the $\text{C}3'-\text{H}3'$ bond interferes with a *syn* N-glycoside conformation which would place atom $\text{O}2$ in close proximity with atom $\text{H}3'$. An *anti* N-glycoside conformation eliminates this apparently unfavourable arrangement. The E_3 conformation is achievable in (I) because it lacks the directing influence of an exocyclic $-\text{CH}_2\text{OH}$. In this ring geometry, the top face of the furanose ring is largely unhindered, allowing the more sterically demanding *syn* geometry about the N-glycoside.

Recent statistical analyses of nucleoside and nucleotide crystal structures (Gelbin *et al.*, 1996) have shown that *N* furanose conformations ($\text{C}3'$ -endo) almost exclusively prefer *anti* N-glycosyl torsions, while *S* forms ($\text{C}2'$ -endo) adopt both *anti* and *syn* geometries. Within the $\text{C}2'$ -endo/*syn* group, virtually all structures were purine nucleosides. In this respect, (I) deviates from expectation. These results suggest that (I) could be useful in the development of NMR probes of N-glycoside conformation [*e.g.* DESERT experiments (Akasaka *et al.*, 1975), with either $\text{H}1'$ or $\text{H}6$ deuterated] or *trans*-glycoside ${}^3J_{\text{C}2',\text{C}2/6}$ studies (Kline & Serianni, 1990), potentially serving as a pyrimidine nucleoside reference structure in which a *syn* N-glycoside may be adopted to some extent in aqueous solution.

The crystal structure of β -erythrouridine, (III), has been reported recently (Czechtizky & Vasella, 2001), and some structural parameters are shown in Table 1. Like (I), the furanose conformation in (III) is E_3 . By comparison, the crystal structure of β -uridine, (IV) (Green *et al.*, 1975), shows 3E conformations for the β -ribofuranose ring in two independent forms. Thus, for pyrimidine nucleosides, the erythro-

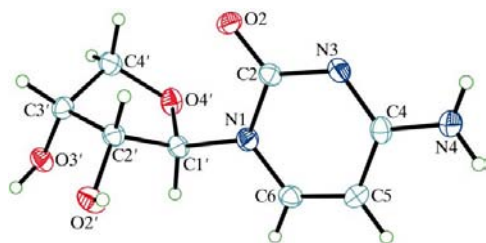


Figure 2

A plot of the molecule of (I). Displacement ellipsoids are drawn at the 50% probability level and H atoms are shown as small spheres of arbitrary radii.

and ribofuranose rings show a consistent difference in their preferred conformation. However, the N-glycoside conformation in (III) is *anti/ac* ($\text{O}4'-\text{C}1'-\text{N}1-\text{C}2 = -131.4^\circ$) (Table 1), unlike that found for (I), and an *anti/ap* N-glycoside conformation is observed in the related compound (IV) ($\text{O}4'-\text{C}1'-\text{N}1-\text{C}2 = -164.41$ and -152.96° in the two forms). Thus, the *syn* conformation observed in (I) may be partly caused by crystal packing forces.

Since the furanose conformations are similar in (I) and (III), the differences in the structural parameters in these structures can be attributed mainly to different N-glycosyl conformations, especially for bond lengths and angles in the vicinity of the anomeric C atom. For example, $r_{\text{C}1',\text{C}2'}$ and the $\text{O}4'-\text{C}1'-\text{N}1$ bond angle are considerably larger in (I) (Table 1). The $\text{C}1'-\text{N}1$ and $\text{C}1'-\text{O}4'$ bond lengths, however, are similar in both structures. It is noteworthy that $r_{\text{C}2',\text{O}2'} < r_{\text{C}3',\text{O}3'}$ in both (I) and (III), whereas these bond lengths are identical in (II). Presumably, the quasi-axial and quasi-equatorial orientations of the $\text{C}3'-\text{O}3'$ and $\text{C}2'-\text{O}2'$ bonds, respectively, in (I) and (III) are responsible for this difference, with the former orientation expected to generate a longer bond (Podlasek *et al.*, 1996). The C—O bond lengths, however, will be modulated by differences in hydrogen bonding in the crystal structures, and these secondary effects may complicate interpretations based solely on bond orientation.

The hydrogen bonding in the crystal structures of (I) and (II) also differs. In (I), atoms $\text{O}2'$ and $\text{O}3'$ each serve as a donor and a mono-acceptor, and atom $\text{O}4'$ is not involved in hydrogen bonding. In (II), atoms $\text{O}2'$, $\text{O}3'$ and $\text{O}4'$ behave similarly, and atom $\text{O}5'$ serves only as a donor. In (III), however, atoms $\text{O}2'$ and $\text{O}3'$ serve only as acceptors, but like (I) and (II), atom $\text{O}4'$ is not involved in hydrogen bonding. In the nitrogen base, the $\text{C}4' \text{NH}_2$ group serves as a donor in two hydrogen bonds, and atom $\text{N}3$ serves as a hydrogen-bond acceptor in both (I) and (II). The $\text{C}2$ carbonyl serves as a single acceptor in (I) and a double acceptor in (II). In (III), the $\text{C}2$ carbonyl serves as a single acceptor, the $\text{C}4$ carbonyl as a dual acceptor, and atom $\text{N}3$ as a donor. An interesting intermolecular hydrogen-bonding pattern is observed in (I), wherein atoms $\text{O}2'$ and $\text{O}3'$ of one molecule serve as donors to

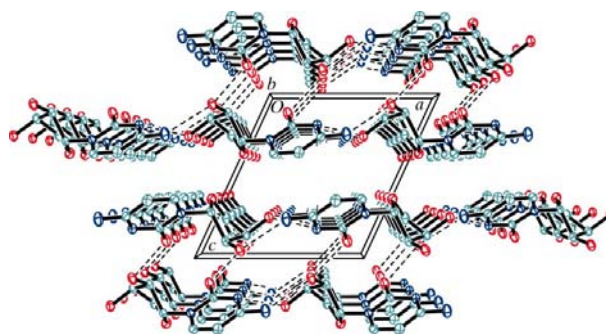


Figure 3

A packing diagram for (I), viewed down the *b* axis, illustrating the hydrogen-bonded bilayers. Dashed lines denote hydrogen bonds.

the C4'-NH₂ and N3 atoms of a second molecule in the crystal lattice. This hydrogen-bonding pattern suggests modes of recognition between nucleosides involving direct base-sugar interactions. This pattern is not observed in (II) and (III).

The structure of (I) forms a hydrogen-bonded bilayer about the *ab* plane (Fig. 3). Each sheet is formed *via* three types of hydrogen bonds, namely N4—H4A···O3'(x + 1, y + 1, z), N4—H4B···O2'(x + 1, y, z) and O3'—H3'···N3(x - 1, y, z). The layers are joined by hydrogen bonding between O2'—H2'O and O2(-x, y + 1/2, -z) of opposite sheets. Details of the hydrogen bonding are summarized in Table 2.

Experimental

Compound (I) was prepared as described previously by Kline & Serianni (1992) and was crystallized from hot ethanol.

Crystal data

C ₈ H ₁₁ N ₃ O ₄	Z = 2
M _r = 213.20	D _x = 1.599 Mg m ⁻³
Monoclinic, P ₂ ₁	Cu Kα radiation
a = 8.5473 (10) Å	μ = 1.11 mm ⁻¹
b = 6.2423 (7) Å	T = 200 (2) K
c = 9.1325 (11) Å	Plate, colourless
β = 114.701 (4)°	0.30 × 0.20 × 0.03 mm
V = 442.68 (9) Å ³	

Data collection

Bruker SMART APEX CCD area-detector diffractometer	5338 measured reflections
φ and ω scans	1269 independent reflections
Absorption correction: multi-scan (Sheldrick, 2004)	1242 reflections with I > 2σ(I)
T _{min} = 0.731, T _{max} = 0.967	R _{int} = 0.023
	θ _{max} = 69.6°

Refinement

Refinement on F ²	w = 1/[σ ² (F _o ²) + (0.0428P) ² + 0.1356P]
R[F ² > 2σ(F ²)] = 0.028	where P = (F _o ² + 2F _c ²)/3
wR(F ²) = 0.076	(Δ/σ) _{max} < 0.001
S = 1.09	Δρ _{max} = 0.24 e Å ⁻³
1269 reflections	Δρ _{min} = -0.21 e Å ⁻³
146 parameters	
H atoms treated by a mixture of independent and constrained refinement	

H atoms attached to carbon were placed at calculated geometries and allowed to ride on the position of the parent atom, with C—H = 0.95–1.00 Å. Hydroxy H atoms were located at the position that maximizes the electron density and this was coupled with a rotating-group refinement; O—H = 0.84 Å. The two H atoms of N4 were located in a difference map and refined freely, including a parameter for isotropic thermal motion, in subsequent cycles of least-squares refinement; N—H = 0.84 (3) and 0.87 (4) Å. For other H atoms, U_{iso}(H) = 1.2U_{eq}(C) or 1.5U_{eq}(O).

Data collection: APEX2 (Bruker, 2006); cell refinement: APEX2 and SAINT (Bruker, 2006); data reduction: SAINT and XPREP (Sheldrick, 2003); program(s) used to solve structure: XS (Sheldrick, 2001); program(s) used to refine structure: XL (Sheldrick, 2001); molecular graphics: XP (Sheldrick, 1998); software used to prepare material for publication: enCIFer (Allen *et al.*, 2004).

The diffractometer was purchased using funds provided by the National Science Foundation (award No. CHE-0443233).

Table 1

Comparison of structural parameters (Å, °) in compounds (I)–(III).

	(I)†	(II)‡	(III)§
C1'—C2'	1.548 (3)	1.534 (5)	1.527
C2'—C3'	1.528 (3)	1.518 (5)	1.525
C3'—C4'	1.512 (3)	1.515 (5)	1.499
C1'—N1	1.475 (2)	1.490 (4)	1.474
C1'—O4'	1.414 (3)	1.409 (4)	1.409
C4'—O4'	1.452 (3)	1.461 (4)	1.445
C2'—O2'	1.414 (3)	1.412 (4)	1.398
C3'—O3'	1.422 (2)	1.412 (4)	1.417
C2—O2/C4—O4	1.234 (3)	1.241 (4)	1.223/1.232
C4—N4	1.335 (3)	1.319 (5)	
C4'—O4'—C1'	108.24 (14)	110.2 (3)	108.7
O4'—C1'—N1	110.56 (16)	108.8 (3)	108.1
O4'—C1'—C2'	107.04 (16)	107.0 (3)	107.6
C1'—C2'—C3'	100.67 (15)	101.1 (3)	102.4
C2'—C3'—C4'	99.78 (15)	102.8 (3)	101.0
C3'—C4'—O4'	104.69 (18)	104.1 (3)	105.9
C1'—N1—C2	121.52 (18)	117.2 (3)	119.1
C1'—N1—C6	117.92 (17)	122.7 (3)	119.1
O4'—C1'—N1—C2	60.8 (2)	-162.6 (3)	-131.4
	(<i>syn</i> ; + <i>sc</i>)	(<i>anti</i> ; <i>ap</i>)	(<i>anti</i> ; - <i>ac</i>)
O4'—C1'—N1—C6	-120.29 (18)	18.1 (4)	46.8
C2'—C1'—N1—C2	-60.6 (3)	79.5 (4)	109.0
C2'—C1'—N1—C6	118.28 (19)	-99.7 (4)	-72.8
C1'—C2'—C3'—C4'	-40.83 (18)	37.6 (3)	-35.1
C2'—C3'—C4'—O4'	42.1	-34.3 (3)	36.6
C3'—C4'—O4'—C1'	26.19 (19)	17.0 (4)	-23.5
C4'—O4'—C1'—C2'	-0.97 (18)	7.3 (4)	0.04
O4'—C1'—C2'—C3'	27.00 (18)	-28.3 (3)	22.6
N1—C2—N3—C4	-4.6 (3)	5.2 (5)	3.9
N1—C6—C5—C4	-2.9 (3)	0.9 (6)	-1.5
Furanose			
P (°)	197.8	7.7 (³ T ₂ ; N)	199.2
	(E ₃ ; C3'- <i>exo</i> ; S)		(E ₃ ; C3'- <i>exo</i> ; S)
τ _m (°)	44	39	38

† Erythrocytidine (this work). ‡ Cytidine (Ward, 1993). § Erythroidine (Czechitzky & Vasella, 2001).

Table 2

Hydrogen-bond geometry (Å, °).

D—H···A	D—H	H···A	D···A	D—H···A
N4—H4A···O3 ⁱⁱ	0.87 (4)	2.20 (4)	2.982 (3)	150 (3)
N4—H4B···O2 ⁱⁱⁱ	0.84 (3)	2.08 (3)	2.912 (3)	177 (2)
O2'—H2'O···O2 ⁱⁱⁱ	0.84	1.88	2.699 (2)	166
O3'—H3'O···N3 ^{iv}	0.84	2.06	2.825 (2)	151

Symmetry codes: (i) x + 1, y + 1, z; (ii) x + 1, y, z; (iii) -x, y + 1/2, -z; (iv) x - 1, y, z.

Supplementary data for this paper are available from the IUCr electronic archives (Reference: GZ3050). Services for accessing these data are described at the back of the journal.

References

- Akasaka, K., Imoto, T., Shibata, S. & Hatano, H. (1975). *J. Magn. Reson.* **18**, 328–343.
- Allen, F. H., Johnson, O., Shields, G. P., Smith, B. R. & Towler, M. (2004). *J. Appl. Cryst.* **37**, 335–338.
- Bruker (2006). APEX2 and SAINT. Bruker AXS Inc., Madison, Wisconsin, USA.
- Czechitzky, W. & Vasella, A. (2001). *Helv. Chim. Acta*, **84**, 1000–1016.

- Flack, H. D. (1983). *Acta Cryst.* **A39**, 876–881.
- Gelbin, A., Schneider, B., Clowney, L., Hsieh, S.-H., Olson, W. K. & Berman, H. M. (1996). *J. Am. Chem. Soc.* **118**, 519–529.
- Green, E. A., Rosenstein, R. D., Shiono, R., Abraham, D. J., Trus, B. L. & Marsh, R. E. (1975). *Acta Cryst.* **B31**, 102–107. (Erratum: *Acta Cryst.* **B31**, 1221.)
- Kempeneers, V., Froeyen, M., Vastmans, K. & Herdewijn, P. (2004). *Chem. Biodivers.* **1**, 112–123.
- Kline, P. C. & Serianni, A. S. (1990). *J. Am. Chem. Soc.* **112**, 7373–7381.
- Kline, P. C. & Serianni, A. S. (1992). *J. Org. Chem.* **57**, 1772–1777.
- Podlasek, C. A., Stripe, W. A., Carmichael, I., Shang, M., Basu, B. & Serianni, A. S. (1996). *J. Am. Chem. Soc.* **118**, 1413–1425.
- Rao, S. T., Westhof, E. & Sundaralingam, M. (1981). *Acta Cryst.* **A37**, 421–425.
- Saenger, W. (1984). *Principles of Nucleic Acid Structure*, pp. 69–78. New York: Springer-Verlag.
- Schoning, K. U., Scholz, P., Guntha, S., Wu, X., Krishnamurthy, R. & Eschenmoser, A. (2000). *Science*, **290**, 1347–1351.
- Sheldrick, G. M. (1998). *XP*. Bruker AXS Inc., Madison, Wisconsin, USA.
- Sheldrick, G. M. (2001). *XL and XS*. Bruker AXS Inc., Madison, Wisconsin, USA.
- Sheldrick, G. M. (2003). *XPREF*. Bruker AXS Inc., Madison, Wisconsin, USA.
- Sheldrick, G. M. (2004). *SADABS*. University of Göttingen, Germany.
- Ward, D. L. (1993). *Acta Cryst.* **C49**, 1789–1792.
- Wilds, C. J., Wawrzak, Z., Krishnamurthy, R., Eschenmoser, A. & Egli, M. (2002). *J. Am. Chem. Soc.* **124**, 13716–13721.